Nanoscale

Accepted Manuscript

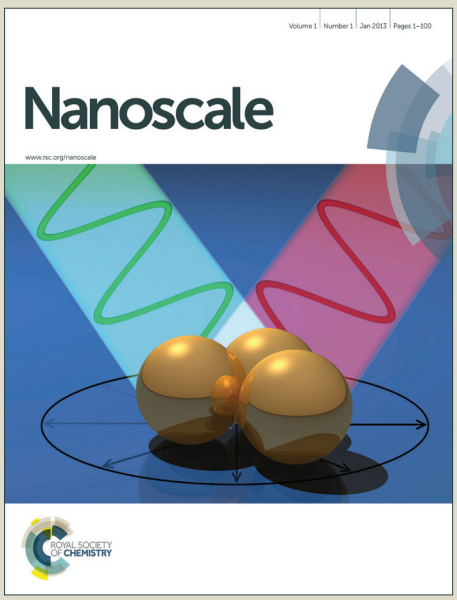

ROYAL SOCIETY OF CHEMISTRY

www.rsc.org/nanoscale

ARTICLE TYPE www. rsc.org/xxxxxx | XXXXXXXX

Superdirective dielectric nanoantenna

Alexander E. Krasnok,*[a] Constantin R. Simovski,[b] Pavel A. Belov [a] and Yuri S. Kivshar[a,c]

We introduce the novel concept of superdirective nanoantennas based on the excitation of higher-order magnetic multipole moments in subwavelength dielectric nanoparticles. Our superdirective nanoantenna is a small Si nanosphere containing a notch, and is excited by a dipole located within the notch. In addition to extraordinary directivity, this nanoantenna demonstrates efficient radiation steering at the nanoscale, resulting from subwavelength sensitivity of the beam radiation direction to variation of the source position inside the notch. We compare our dielectric nanoantenna with a plasmonic nanoantenna of similar geometry, and reveal that the nanoantenna's high directivity in the regime of transmission is not associated with strong localization of near fields in the regime of reception. Likewise, the absence of hot spots inside the nanoantenna leads to low dissipation in the radiation regime, so that our dielectric nanoantenna has significantly smaller losses and high radiation efficiency of up to 70 %.

1 Introduction

Nanoantennas have become a subject of considerable interest with numerous stunning applications in optical and quantum communications, nonlinear optics, sensing, and photovoltaics[1–7]. A transmitting nanoantenna effectively converts a localized electromagnetic field into freely propagating light. A receiving nanoantenna performs the inverse transformation. Efficiency of this light transformation process is basically characterized by the Purcell factor and coefficient of local field enhancement for transmitting and receiving nanoantennas, respectively.

The far-zone electromagnetic radiation is a transverse wave in which the the electric field $\mathbf{E}$, magnetic field $\mathbf{H}$ and wave vector $\mathbf{k}$ are mutually orthogonal. In this case the following equation holds $\mathbf{E} = \mathrm{Z}_0\,(\mathbf{k}\times\mathbf{H})$, where $Z_0 = 120\pi$ Ohm[8] is a fundamental physical constant called the impedance of free space. On the other hand the impedance of quantum light sources is characterized by the von Klitzing constant $\mathrm{R}_k = h/e^2 \simeq 25$ kOhm[9]. The ratio of these two values $\mathrm{Z}_0/\mathrm{R}_k = 1/137$ is called the fine-structure factor. The low value of this constant means a that objects comparable in size to the de Broglie wavelength interact very weakly with light. This is the case, for example, in quantum dots. In spite of the importance of quantum dots and other quantum sources in modern optics, they are very inefficient as sources of light because their impedances are mismatched with the impedance of free space. For this reason optical nanoantennas are introduced to effectively match the impedance of a quantum source to free space, greatly increasing the efficiency of radiation and excitation by light.

[a] *National Research University of Information Technologies, Mechanics and Optics, St. Petersburg 197101, Russia; E-mail: krasnokfiz@mail.ru*
[b] *Aalto University, School of Electric and Electronic Engineering, Aalto FI76000, Finland*
[c] *Nonlinear Physics Center, Research School of Physics and Engineering, Australian National University, Canberra ACT 0200, Australia*

Another characteristic of nanoantennas, besides their efficiency, is the directionality, i.e. the enhancement of transmission and reception of light in a desired direction. Directionality of the antenna radiation and reception are both characterized by the directivity factor: $\mathrm{D}(\theta,\phi) = 4\pi\mathrm{P}(\theta,\phi)/\mathrm{P}_{\mathrm{tot}}$, where $\mathrm{P}(\theta,\phi)$ is the power density of radiation in the direction (θ,ϕ), $\mathrm{P}_{\mathrm{tot}}$ determines the total radiated power in all directions and (θ,ϕ) are the angular spherical coordinates. For subwavelength nanoantennas dominated by a single electric or a magnetic dipole moment the directivity is 1.5. For a fixed wavelength this parameter is proportional to the size of the nanoantenna. High directivity (of the order of 10) is usually achieved at the expense of the optically large size of the nanoantenna (its length or its geometric aperture).

Why the creation of a high directive radiating system is a significant problem in the theory of nanoantennas? In the optical frequency range highly directional nanoantennas are required for optical wireless nanolink systems[2,5,10,11]. Furthermore, highly directional nanoantennas can solve the problem of collecting the energy radiated by a single quantum emitter, for example a quantum dot or nitrogen-vacancy center, to create an effective single-photon source. Additionally, a highly directional receiving nanoantenna is a powerful tool which allows very high values for the local field gradient to be achieved. The field variation on the subwavelength scale is useful to control the dynamics of the states of quantum sources. In nanophotonics, directivity sufficiently high for these purposes has been theoretically and experimentally achieved for arrayed plasmonic antennas utilizing the Yagi-Uda design approach[4,5,12–14]. Also, large dielectric spheres[15], and metascreens[16] allow high directivity of nanoantennas in the optical range. In all of these cases, while individual elements of these arrays are subwavelength, the overall size of the radiating system turns out to be greater than the radiation wavelength λ.

In the classical theory of antennas a fundamentally differ-

ent approach to creating a high directivity is known. This approach is based on creating rapidly spatially-oscillating currents in a subwavelength area, which leads to higher multipole moments being excited in the antenna system. As a result, the antenna becomes directive in spite of its subwavelength volume, or, in the language of radio engineers, *superdirective*. *Superdirectivity is defined as a significant enhancement of directivity of a subwavelength antenna system relative to the directivity of a point dipole*[8,17–19]. The directivity of superdirective microwave antennas is usually $\simeq 10$[17,20]. Larger values are rarely used due to the high dissipative losses.

Recently, magnetic resonances of high-index dielectric nanoparticles were investigated theoretically and experimentally for the enhancement of nanoantenna directivity[13,21,22]. High-permittivity nanoparticles can have electric and magnetic dipole responses which are both near resonance and of the same magnitude and phase[7,13,22–26]. The balance of the electric and magnetic dipoles oscillating with the same phase allows the practical realization of a Huygens source, an elementary emitting system with a cardioid pattern[8,13,21,23] and with a directivity of ~3.5. Superdirectivity requires a directivity higher than this, with the condition that the maximal size of the antenna system does not exceed half the wavelength.

Note that the excitation of a magnetic dipole resonance in a subwavelength nanosphere leads to improved directionality without a significant increase of the antenna size. Furthermore, in Ref.[27] it is shown that the excitation of a magnetic quadrupolar mode in a dielectric nanosphere leads to an increase of the directivity compared to that of the magnetic or electric dipole. This indicates that high-order multipole moments excited in a subwavelength particle may result in superdirective radiation when the particle is excited by a nearby quantum source, and superdirective reception of incoming light. However, the question remains as to how higher-order multipoles can be excited in a subwavelength particle.

In this paper, we employ high-permittivity dielectric nanoparticles of subwavelength size, where a high-order magnetic multipole response is induced by a very inhomogeneous external field, resulting in superdirectivity. We consider a dielectric nanosphere of size 0.3-0.5λ having a notch, excited by a point emitter located within the notch. This geometry is similar to the so-called plasmonic nanocup resonator [28–31]. The non-uniformity of the applied field is enhanced by the notch, transforming the energy of the magnetic-dipole Mie resonance normally generated in the sphere into high-order multipole moments, where the magnetic multipoles dominate over the electric ones. Our system is very different from known dielectric lenses and cavities which are large compared to the wavelength. Another important feature of the notched dielectric resonator is the huge sensitivity of the radiation direction to the spatial position of the emitter inside the notch. This property allows efficient beam steering and measuring the location

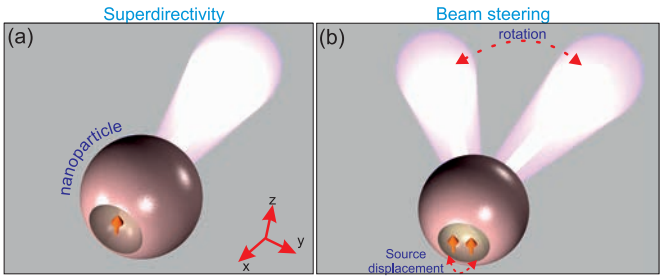

Fig. 1 (a) Geometry of a superdirective dielectric nanoantenna excited by a point-like dipole. (b) Concept of the beam steering effect at nanoscale.

of a quantum source with strongly subwavelength precision via the detected radiation direction. The proposed design of superdirective nanoantennas may also be useful for collecting single photon emission, monitoring the states of quantum objects, and nanoscale microscopy. In this paper, we study only the most interesting effect, superdirectivity, leaving aside issues related to the Purcell factor of our nanoantenna. This is remarkably different from the coefficient of local field enhancement in the receiving regime, discussion of which we defer to a subsequent work.

Subwavelength spatial oscillations of the radiating currents which are needed to achieve superdirectivity imply that near fields of the nanoantenna become strongly inhomogeneous, and the near-field zone must extend further than that of a point dipole. This results in an increase of the effective aperture area $S = D_{max}\lambda^2/(4\pi)$, which is associated with the maximum directivity $D_{max} = 4\pi P_{max}/P_{tot}$, where λ is the wavelength in the environment in which the antenna radiates (free space in our case) and P_{max} is the power density in the direction of maximum radiation. Normalizing the effective aperture S by the geometric aperture of a spherical antenna $S_0 = \pi R_S^2$, we obtain the normalized effective aperture S_n in the form:

$$S_n = \frac{D_{max}\lambda^2}{4\pi^2 R_S^2} \gg 1. \quad (1)$$

In practice, $S_n = 4\ldots5$ is sufficient for superdirectivity of a subwavelength sphere. In this work, we theoretically demonstrate a nanoantenna with $S_n = 6.5$ in the visible range.

2 Superdirective dielectric nanoantenna

Here we show the practical possibility to create a superdirective nanoantenna without utilizing plasmonic arrays or the hypothetical metamaterials discussed in Ref.[32]. We consider a silicon nanoparticle, taking into account the frequency dispersion of the dielectric permittivity and optical losses[33]. In our example the radius of the silicon sphere is $R_S = 90$ nm. For

a simple sphere under homogeneous (e.g. plane-wave) excitation, electric and magnetic dipoles can be resonantly excited while the contribution of higher-order multipoles is negligible [13]. Making a notch in the sphere breaks the symmetry and increases the contribution of higher-order multipoles to scattering, even if the sphere is still excited homogeneously. Further, by placing a nanoemitter (e.g. a quantum dot) inside the notch, as shown in Fig.1, we create the conditions for the resonant excitation of multipoles: the field exciting the resonator is now spatially very non-uniform, thus it has strong overlap with high order multipole moments. In principle, the notched particle operating as a nanoantenna can be formed from a variety of semiconductor materials and can have various shapes – spherical, ellipsoidal, cubic or conical. However, in this work, the particle is a silicon sphere and the notch has the shape of a hemisphere with radius $R_n < R_S$. The emitter is modeled as a point-like dipole and is shown in Fig.1 by a red arrow.

It is important to distinguish our approach from the apparently similar one presented in Refs. [34,35], where a small notch on the surface of a semiconductor microlaser was used to achieve higher emission directivity by modifying the field distribution inside the resonator [36]. Unlike the work presented here, these earlier structures are not subwavelength and therefore their directive emission is not related to superdirectivity. In our case, the nanoparticle is much smaller than the wavelength. For the same reason our nanoantenna is quite distinct from dielectric [37,38] or Luneburg [39,40] lenses. The smallest known dielectric lenses are immersion lenses [41–44], but their sizes are at least 1-2 μm for operation in the visible frequency range. The function of such lenses is to collect radiation using a large geometric aperture S, while $S_n \simeq 1$. Our approach demonstrates that a subwavelength system with small *geometric aperture* can have high directivity due to an increase of the *effective* aperture. Furthermore, the idea of shape changing of a plasmon nanoantenna has already been used for optimization of the transmission spectrum [45] First, we consider a particle without a notch, excited inhomogeneously by a point emitter. To study the problem numerically, we employed the simulation software CST Microwave Studio. Fig.2a shows the dependence of the maximum directivity D_{max} on the position of the source in the case of a sphere with $R_S = 90$ nm and no notch, at the wavelength $\lambda = 455$ nm (blue curve with crosses). This dependence has maximum ($D_{max} = 7.1$) when the emitter is placed inside the particle at the distance 20 nm from its surface. The analysis shows that in this case the electric field distribution inside the particle corresponds to the significant excitation of higher-order multipole momoments, which is not achievable with homogeneous excitation. In this way, superdirectivity can be achieved, even without the notch. Due to the very close location of the point source, the external field is so inhomogeneous that the magnetic and electric dipole components of the polarization current in the sphere

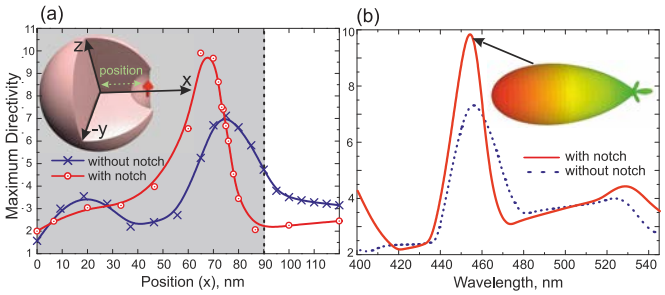

Fig. 2 (a) Maximum of directivity depending on the position of the emitter ($\lambda = 455$ nm) in the case of a sphere with and without a notch. Vertical dashed line marks the particle radius centered at the coordinate system. (b) Directivity dependence on the radiation wavelength. The inset shows three-dimensional radiation pattern of the structure ($R_S = 90$ nm and $R_n = 40$ nm).

are no longer dominant, as they would be when the sphere is excited by a plane wave.

By creating a small notch around the emitter we significantly enhance the amplitudes of the high-order multipoles, as is shown in Fig.1. This geometry transforms the sphere into a resonator with significant high-order multipole moments. In this example the center of the notch is exactly on the nanosphere's surface, which most likely corresponds to the maximal directivity configuration for an emitter located inside the notch. Moreover, the location of the source inside the particles is a very difficult experimental task and the presence of the notch simplifies the practical application of this nanoantenna.

The optimal radius of the notch for maximal directivity in this example is $R_n = 40$ nm. In Fig.2a the interpolated red curve with circles corresponds to the simulation results, and shows the maximal directivity versus the location of the emitter at the wavelength 455 nm. The maximal directivity $D_{max} = 10$ is achieved at this wavelength as one can see from Fig.2b, which shows the directivity versus λ with and without a notch. The inset shows the three-dimensional radiation pattern of the structure at λ =455 nm. The main lobe of this pattern has an angular width (3 dB below the maximum) of 40°. This value of directivity corresponds to the normalized effective aperture $S_n = 6.5$. Fig.3a,b show the distribution of the magnitude and phase of the electric field inside and in the vicinity of the nanoantenna. The electric field inside the particle is strongly inhomogeneous at λ =455 nm i.e. in the regime of maximal directivity (the same holds for the magnetic field, as shown in Fig.3c,d). In this regime, the internal area where the electric field oscillates with approximately the same phase turns out to be maximal. This area is located within the spherical particle on the side opposite to the notch, as can be seen in Fig.3b,d. In other words, the effective near zone of the nanoantenna in the superdirective regime is maximal.

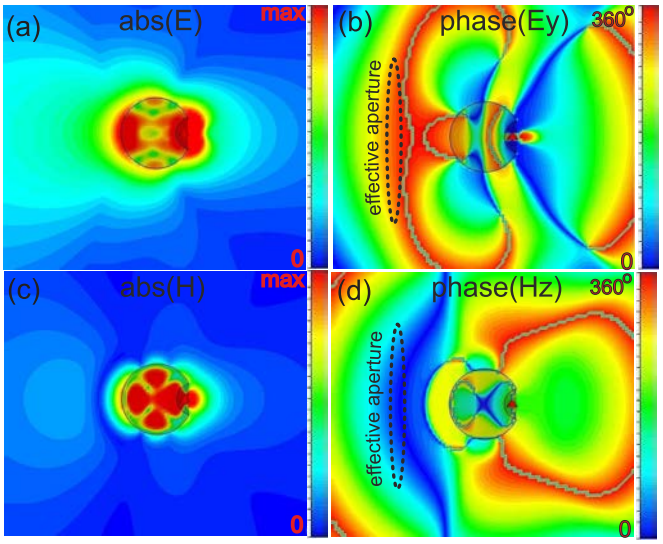

Fig. 3 Distribution of (a) absolute value and (b) phase of the electric field (c and d for the magnetic field, respectively) of the all-dielectric superdirective nanoantenna with the source in the center of the notch, at the wavelength $\lambda = 455$ nm.

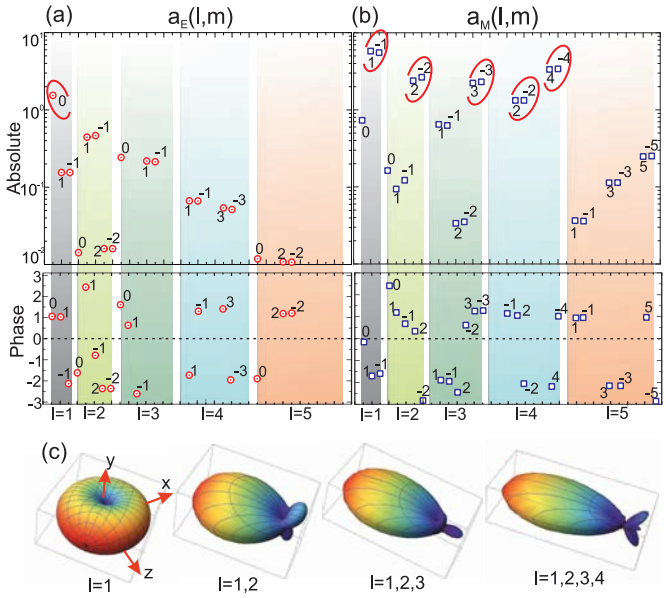

Fig. 4 Magnitude and phase of (a) electric and (b) magnetic multipole moments that provide the main contribution to the radiation of the all-dielectric superdirective optical nanoantenna at the wavelength 455 nm. Multipole coefficients providing the largest contribution to the antenna directivity are highlighted by red circles. (c) Dependence of the radiation pattern of all-dielectric superdirective nanoantenna on the number of multipoles taken into account. The dipole like source is oriented along the z axis.

Next, we demonstrate how to find the multipole moments excited in the all-dielectric superdirective nanoantenna which are responsible for its enhanced directivity. The internal field is obtained from numerical simulation, and yields the polarization currents in the nanoparticle, which we expand into multipole moments following [46]. The expansion is a series of spherical harmonics with coefficients $a_E(l,m)$ and $a_M(l,m)$, which characterize the electrical and magnetic multipole moments respectively [46]:

$$\begin{aligned} a_E(l,m) &= \frac{4\pi k^2}{i\sqrt{l(l+1)}} \times \\ &\int Y^*_{lm}\left(\rho\frac{\partial}{\partial r}[r j_l(kr)] + \frac{ik}{c}(\mathbf{r}\cdot\mathbf{j}) j_l(kr)\right) d^3x, \\ a_M(l,m) &= \frac{4\pi k^2}{i\sqrt{l(l+1)}} \int Y^*_{lm} \mathrm{div}\left(\frac{\mathbf{r}\times\mathbf{j}}{c}\right) j_l(kr) d^3x, \quad (2) \end{aligned}$$

where $\rho = 1/(4\pi)\mathrm{div}\mathbf{E}$ and $\mathbf{j} = c/(4\pi)(\mathrm{rot}\mathbf{H} + ik\mathbf{E})$ are densities of the *total* electric charges and currents that can be easily expressed through the internal electric $\mathbf{E}$ and magnetic $\mathbf{H}$ fields of the sphere, Y_{lm} are spherical harmonics of order $(l > 0, 0 \geq |m| \leq l)$, $k = 2\pi/\lambda$, $j_l(kr)$ is the spherical Bessel function of order l and c is the speed of light. The coefficients $a_E(l,m)$ and $a_M(l,m)$ determine the electric and magnetic multipole moments, namely dipole at $l = 1$, quadrupole at $l = 2$, octupole at $l = 3$ etc.

The multipole coefficients determine not only the mode structure of the internal field but also the angular distribution of the radiation. In particular, in the far field zone electric and magnetic fields of multipole order l depend on the distance r as [46] $\sim (-1)^{i+1}\frac{\exp(ikr)}{kr}$ and the expression for the angular distribution of radiated power can be written as follows:

$$\begin{aligned} \frac{\mathrm{d}P(\theta,\varphi)}{\mathrm{d}\Omega} &= \frac{c}{8\pi k^2} \times \\ &\left|\sum_{l,m}(-i)^{l+1}[a_E(l,m)\mathbf{X}_{lm}\times\mathbf{n} + a_M(l,m)\mathbf{X}_{lm}]\right|^2, \\ \mathbf{X}_{lm}(\theta,\varphi) &= \frac{1}{\sqrt{l(l+1)}}\begin{bmatrix} A^-_{l,m}Y_{l,m+1} + A^+_{l,m}Y_{l,m-1} \\ -iA^-_{l,m}Y_{l,m+1} + iA^+_{l,m}Y_{l,m-1} \\ mY_{l,m} \end{bmatrix}, \quad (3) \end{aligned}$$

where $A^{\pm}_{l,m} = (1/2)\sqrt{(l\pm m)(l\mp m+1)}$, $\mathrm{d}\Omega = \sin(\theta)\mathrm{d}\theta\mathrm{d}\varphi$ is the solid angle element in spherical coordinates and $\mathbf{n}$ is the unit vector from the origin to the observation point. The coefficients $a_E(l,m)$ and $a_M(l,m)$ are normalized such that for a given amplitude they contribute equally to the total radiated power. Since in most subwavelength systems higher-order multipoles have negligibly small amplitudes compared to $a_E(1,m)$ and $a_M(1,m)$, they are not usually considered. The multipole moments are found by using the expressions (2) with the electric and magnetic field distributions shown in Fig.3a-d. The amplitudes of the multipole moments

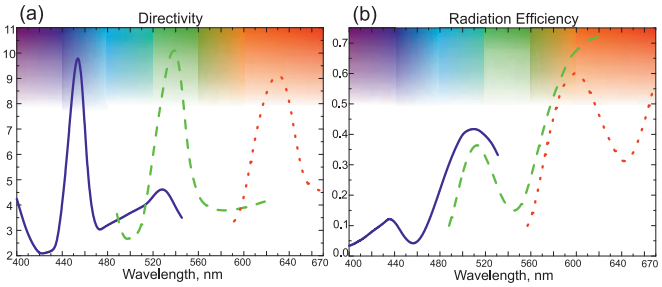

Fig. 5 Dependence of directivity (a) and radiation efficiency (b) on the size of the nanoantenna. Here, the blue solid lines correspond to the geometry – $R_S = 90$ nm, $R_n = 40$ nm, the green dashed curves – $R_S = 120$ nm, $R_n = 55$ nm and the red dotted curves – $R_S = 150$ nm, $R_n = 65$ nm. The nanoantenna efficiency due grows to the reduction of dissipative losses in silicon with increasing wavelength.

are shown in Fig.4, where we observe strong excitation of $a_E(1,0)$, $a_M(1,1)$, $a_M(1,-1)$, $a_M(2,2)$, $a_M(2,-2)$, $a_M(3,3)$, $a_M(3,-3)$, $a_M(4,2)$, $a_M(4,-2)$, $a_M(4,4)$ and $a_M(4,-4)$. These multipole moments determine the angular pattern of the antenna. All others give negligible contributions. The absolute values of all magnetic moments are larger than those of the electric moments of the corresponding order, and the effective spectrum of magnetic multipoles is also broader than that of the electric moments. Thus, the operation of the antenna is mainly determined by the magnetic multipole response. The absolute values of multipole coefficients $a_M(l,\pm|m|)$ of the same order l are practically equivalent, however, the phases of some coefficients differ. Therefore, the modes with $+|m|$ and $-|m|$ create strong anisotropy between the forward and backward directions, resulting in unidirectional radiation.

We have transformed the multipole coefficients into an angular distribution of radiation in accordance with (3) by using the distribution of electric and magnetic fields in Fig.3a-d and determining the relative contribution of each order l. Fig.4c shows how the directivity grows as higher order multipoles terms are added to the response. The right panel of Fig.4c corresponds closely to the inset in Fig.2.

Generally, the superdirectivity effect is accompanied by a significant increase of the effective near field zone of the antenna compared to that of a point dipole for which the near zone radius is equal $\lambda/2\pi$. In the optical frequency range this effect is especially important, considering the crucial role of near fields at the nanoscale.

We consider now the possibility of experimental realization of our superdirective nanoantenna. There are a number of works where structures have already been implemented at the nanoscale. For example, similarly shaped particles to that considered in this article were experimentally fabricated by controlled deformation of a spherical shell[47–49]. By using the same type of instability it is possible to produce colloids of more complex shape with notches and to form clusters[50]. The recent experimental progress in nanoshells and semishells seems to be very promising to produce such nanoantennas[51]. These methods have already been used for the production of plasmonic nanoantennas of similar geometry[28–31].

2.1 Radiation efficiency

Usually, the superdirective regime corresponds to a strong increase of dissipative losses[8]. The radiation efficiency of the nanoantenna is determined by $\eta_{rad} = P_{rad}/(P_{rad} + P_{loss})$, where P_{loss} is the power dissipated through losses in the nanoantenna. However, the multipole moments excited in our nanoantenna are mainly of the magnetic type. This leads to a dominance of the magnetic near field over the electric one. Since the dielectric material does not dissipate magnetic energy, the effect of superdirectivity does not lead to such a large increase of losses in our nanoantenna as would be the case for dominating electric multipoles. If we compare our nanoantenna with a plasmonic nanoantenna, which is the most popular type of nanoantenna due to the relatively strong plasmon resonance, the advantage of our structure becomes evident a priori. The high directivity of plasmonic nanoantennas is achieved by excitation of higher *electric* multipole moments in plasmonic nanoparticles[52–54]. One exception is the directivity of core-shell resonators consisting of a plasmonic material and a hypothetical metamaterial which would demonstrate the extreme material properties in the nanoscale[32]. In all of these cases resonant losses are unavoidable. Moreover, the values of directivity achieved for such nanoantennas do not correspond to superdirectivity, since they are not subwavelength.

Unfortunately, since the electric near field is non-zero the losses in our nanoantenna are not negligible if it operates in the visible range. At wavelengths 440-460 nm (blue light) the directivity achieves 10 but the radiation efficiency is smaller than 0.1 (see Fig.5). This is due to the high losses of silicon in this range[33]. The peak of directivity is shifted to longer wavelengths with increasing size of the nanoantenna. For the design parameters corresponding to the operating wavelength of 630 nm (red light) the calculated value of radiation efficiency is rather high at 0.5, with nearly same directivity close to 10. This is a very good result for the superdirective antenna which has not been demonstrated previously even in theoretical works. There are high dielectric permittivity materials in the infrared range, such as Si, AlSb, GaSb, with even lower losses, which allow the efficiency to achieve 0.7 whilst maintaining high directivity.

We emphasize that the proposed superdirectivity effect is not achieved at the cost of increased losses. This is an important advantage compared to superdirective radio-frequency antenna arrays[8,17–19] and compared to their possible optical analogues – compact arrays of plasmonic nanoantennas with

phase distribution controlled by some mechanism.

2.2 Steering of light at the nanoscale

Here we examine the response of the nanoantenna to subwavelength displacement of the emitter. Displacement along the y axis leads to rotation of the beam *without reducing the superdirectivity*. Fig.6a shows the radiation patterns of the antenna with the source in the center (solid line) and the rotation of the beam for a 20 nm left/right offset (dashed lines). Shifting the source to the right side leads to a rotation of the pattern to the left, and vice versa. The angle of the beam rotation is equal to 20 degrees. The result depends on the geometry of the notch, and is strong enough that it should be readily observable in experiments. For a hemispherical notch, the dependence of the rotation angle on the displacement is presented in Fig.6b.

To interpret the beam steering effect, consider the expansion of the field in electric and magnetic multipoles, as shown in Fig.7. In the case of asymmetric location of the source in the notch (a 20 nm offset to the left) the absolute values of $a_M(l,\pm|m|)$ are different. This means that the moment $a_M(l,+|m|)$ is excited more strongly than $a_M(l,-|m|)$, or vice versa, depending on the direction of displacement. The effect of superdirectivity remains for all values of source offset up to the edge of notch. Small displacements of the source along x and z do not lead to rotation of the pattern. Instead of the movement of a single quantum dot one can consider the emission of two or more quantum dots located near the edges of the notch. In this case, the dynamics of their spontaneous decay will be clearly displayed in the angular distribution of the radiation. This can be useful for quantum information processing and for biomedical applications.

The beam steering effect described above is similar to the effect of beam rotation in the hyperlens[55–57], where the displacement of a point-like source leads to a change of the angular distribution of the radiated power. Switching of the surface wave direction by changing the excitation polarization was theoretically and experimentally realized[58]. However, in our case, the nanoantenna has subwavelength dimensions and therefore it cannot be classified as a hyperlens nor as a microspherical dielectric nanoscope [37,38]. Moreover it is not an analogue of solid immersion micro-lenses [41–44], which are characterized by a size of 1-5 μm in the same frequency range. These lenses have subwavelength resolving power due to their large geometric apertures but have normalized effective apertures $S_n \simeq 1$. Our study demonstrates that the sub-wavelength system, with geometric aperture *small compared to the wavelength* can have both high directivity and high resolving power *because of the strong increase of the effective aperture compared to the geometric one*.

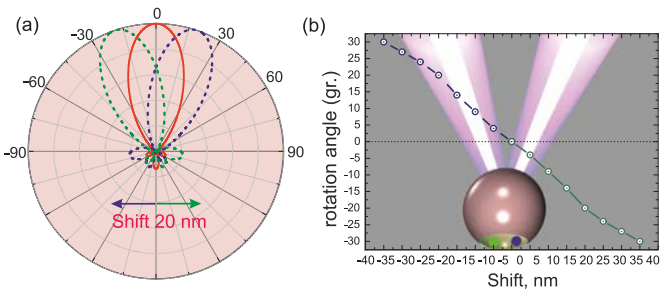

Fig. 6 The rotation of the main beam of the radiation pattern, with subwavelength displacement of the emitter inside the notch. (a) The radiation pattern of the antenna with the source in the center (solid line) and the rotation of the beam radiation pattern for the 20 nm left/right offset (dashed lines). (b) Dependence of the the rotation angle on the source offset.

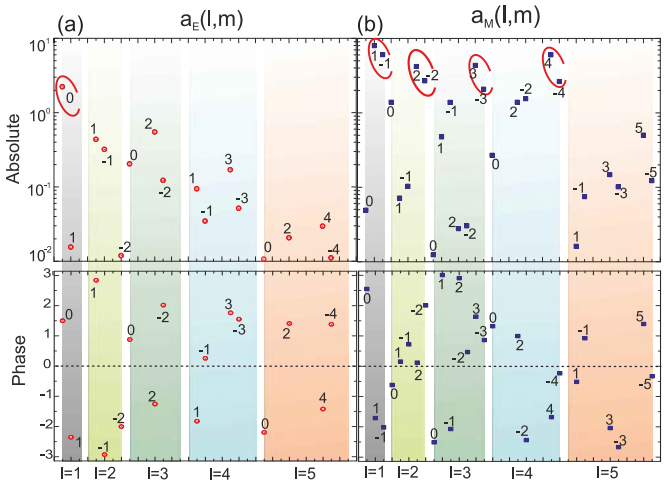

Fig. 7 Absolute values and phases of (a) electric and (b) magnetic multipole moments that provide the main contribution to the radiation of the all-dielectric superdirective optical nanoantenna in the case of asymmetric location of the source at the wavelength 455 nm. The coefficients that give the largest contribution to the antenna directivity are highlighted by red circles.

3 Comparison with plasmonic nanoantennas

To be more convincing in our claims we theoretically demonstrate that superdirectivity only appears in the case of a dielectric nanosphere and does not appear if it is replaced by its plasmonic analogue. To do this, we have studied the directivity as a function of wavelength for the same geometry with a notch (see Fig.2) but made from metal. We considered both silver (Ag) and gold (Au) notched nanospheres. The calculations were performed in a wider wavelength range than in the case of a dielectric nanoantenna, and for several positions of the point source. Results are shown in Fig.8a,c. In

all cases the superdirectivity is not observed. We studied the directivity of a metal nanoantenna with a notch for different sizes of the nanosphere (up to a half-wavelength in diameter). It was found that the geometry of the notch plays a minor role. The directivity never exceeds 4. This clearly demonstrates that the effect of superdirectivity in such a system requires transparency of the nanoantenna material.

Also in the case of metal nanoparticles, when placing the source into the cavity, the dissipative losses increase dramatically (see Fig.8b,d). This is due to the strong electric field penetration into the plasmonic nanoparticles. At the same time a significant part of the volume of the metal nanoparticles is not polarized and the angular distribution of the radiation in the far zone is determined by the radiative losses of surface plasmon modes. We note that these results do not mean that the superdirectivity effect is fundamentally impossible for plasmonic nanoantennas.

4 Receiving regime of nanoantennas

Finally, we consider the superdirective dielectric nanoantenna operating in the receiving regime. Here we show that the high directivity of our nanoantenna in the transmitting mode is not associated with high local field enhancement in the receiving regime, in contrast to lens antennas. The magnitude of the electric field of the all-dielectric superdirective nanoantenna is depicted in Fig.9a, for excitation by a plane wave of wavelength $\lambda = 455$ nm. The direction of **k** of the incident

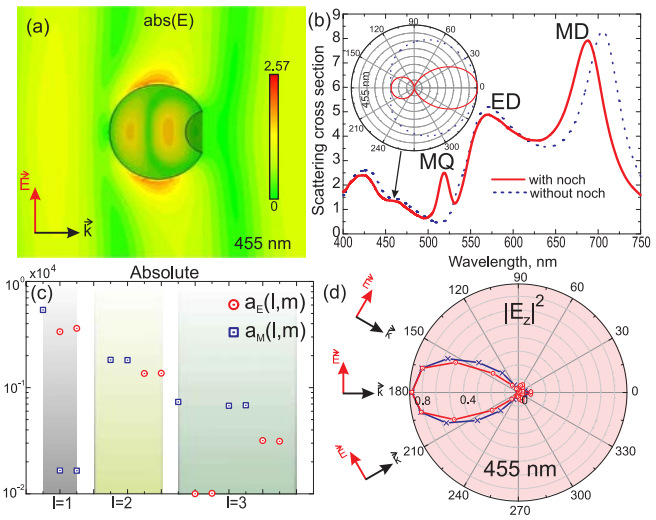

Fig. 9 (a) Absolute values of the electric field of the all-dielectric superdirective nanoantenna for the case of plane wave excitation. The amplitude of the incident electric field is 1. (b) Dependence of the total cross section (normalized to πR_s) on the light wavelength for the nanoparticle without (blue, dashed line) and with (red, solid line) the notch. (c) Absolute values of electric and magnetic multipole moments for plane wave excitation. (d) The intensity of the z component of electric field (i.e. $|E_z|^2$) as a function of the angle of incidence in the E (red curve) and H (blue curve) planes. Figures a,c,d correspond to the wavelength $\lambda = 455$ nm.

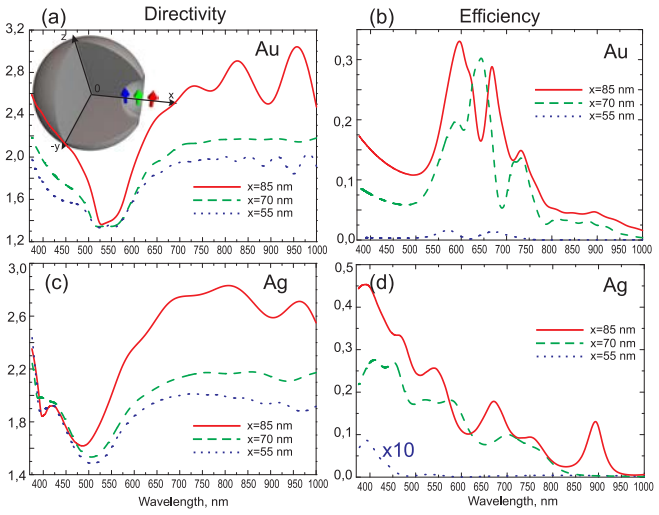

Fig. 8 Dependence of directivity and radiation efficiency on the light wavelength for gold (a,b) and silver (c,d) plasmonic nanoantennas, respectively. The geometric parameters correspond to Fig.2. The dielectric constants of gold and silver are taken from Johnson and Christy's experimental data [59].

wave is opposite to the maximum directivity direction in the transmitting regime. The maximum coefficient of the local field enhancement is only 2.57, so there are no hot spots in which the absorption of incident energy is strongly enhanced. Fig.9b shows the dependency of the scattering cross section normalized to πR_s as a function of the light wavelength for the nanoparticle without and with notch. This figure shows that the nanoparticle does not exhibit a resonant response near the operating wavelength and the presence of the notch has almost no effect on the scattering cross section and the directivity patterns. Peaks MD, ED and MQ corresponds to magnetic dipole, electric dipole and magnetic quadrupole resonances, respectively. Fig.9c shows the mode composition of the field for the case of plane wave excitation. The dipole and quadrupole modes are dominant but not resonant. The high directivity of our notched sphere in the transmitting regime does not imply hot spots inside the sphere in the receiving regime. In accordance with reciprocity, it implies a significant variation of local fields depending on the incident angle. In the case of a point dipole source which is oriented along the z axis the reciprocity theorem gives the following expression[4,5] for the intensity of the z component of the electric field for unit

external field strength:

$$|E_z|^2(\theta,\phi) = \frac{2}{3}\Gamma_{\rm rad}{\rm D}(\theta,\phi), \quad (4)$$

where the directivity of a point dipole in free space is $D(\theta,\phi) = 3/2\sin^2(\theta)$ and $\Gamma_{\rm rad} = P_{\rm rad}/P^0_{\rm rad}$. It represents the relation between the emission of a point dipole in the presence of the nanoantenna $P_{\rm rad}$ and in its absence $P^0_{\rm rad}$, i.e. it is the radiative part of the Purcell factor. Expression (4) shows that the angular dependence of the intensity of the z component of the local electric field at the location of the point source coincides with the directivity pattern of the nanoantenna in transmission mode. Indeed, Fig.9d shows $|E_z|^2$ as a function of the angle of incidence. The power absorbed by a receiving point dipole is proportional to $|E_z|^2$ at its location, with the coefficient of proportionality being the polarizability of the dipole, which is independent of the angle of incidence. The diagram in Fig.9d shows that the absorbed power has an extreme dependence on the angle of incidence. When changing the angle of incidence by 30° from the direction of maximum absorption the absorption reduces by 50%. Furthermore, the ratio of the absorbed power in the backward 180° and forward 0° directions is 8. In between there are directions of the external wave for which the nanoantenna has almost no absorption, emulating an ideal scatterer such as a perfect conductor. Note also that the low value of $|E_z|^2$ along with the high directivity of the nanoantenna mean that the factor $\Gamma_{\rm rad}$ is small. However, this factor can be increased considerably by using a dimer of two plasmonic nanoparticles, as in Ref. [15].

5 Conclusions

We proposed a novel approach for achieving superdirectivity of optical nanoantennas. We studied theoretically the radiation properties of a small high-index dielectric nanoparticle with a notch and demonstrated that a point emitter (such as a quantum dot) placed in the notch efficiently excites higher-order magnetic multipole moments. These magnetic moments are responsible for the high directivity of the subwavelength nanoantenna, exceeding that achievable by any other method. We explained this effect via the enhancement of the effective radiation aperture. In contrast to conventional optical antennas, our design has significantly smaller losses and extraordinary radiation efficiency of up to 70 %. We have also discovered an efficient beam-steering effect when the position of the subwavelength source is offset. The combination of superdirectivity with the beam steering capability makes our results very promising for several applications in nanophotonics. Furthermore, we compared our all-dielectric nanoantennas with plasmonic nanoantennas of the same geometry, and found the superdirectivity effect to be absent in these plasmonic structures. We showed that the high directivity of our nanoantenna in the transmission regime is not associated with strong localization of the near field and therefore with high losses in the reception regime.

References

1 H. Giessen and M. Lippitz, *Science*, 2010, **329**, 910.
2 N. J. Halas, *PNAS*, 2010, **106**, 3643–3644.
3 A. G. Curto, G. Volpe, T. H. Taminiau, M. P. Kreuzer, R. Quidant and N. F. van Hulst, *Science*, 2010, **329**, 930.
4 L. Novotny and N. van Hulst, *Nat. Photon.*, 2011, **5**, 83–90.
5 P. Biagioni, J. Huang and B. Hecht, *Rep. Prog. Phys.*, 2012, **75**, 024402.
6 N. Berkovitch, P. Ginzburg and M. Orenstein, *J. Phys.: Condens. Matter*, 2012, **24**, 073202.
7 A. E. Krasnok, I. S. Maksymov, A. I. Denisyuk, P. A. Belov, A. E. Miroshnichenko, C. R. Simovski and Y. S. Kivshar, *Phys.-Usp.*, 2013, **56**, 539–564.
8 C. Balanis, *Antenna Theory: Analysis and Design*, New York ; Wiley, 1982.
9 M. D. Ventra, *Electrical transport in nanoscale systems*, Cambridge University Press, 2006.
10 A. Alu and N. Engheta, *Phys. Rev. Lett.*, 2010, **104**, 213902.
11 D. M. Solis, J. M. Taboada, F. Obelleiro and L. Landesa, *Optics Express*, 2013, **21**, 2369.
12 D. Dregely, R. Taubert, J. Dorfmuller, R. Vogelgesang, K. Kern and H. Giessen, *Nat. Comm.*, 2011, **2**, 267.
13 A. E. Krasnok, A. E. Miroshnichenko, P. A. Belov and Y. S. Kivshar, *Optics Express*, 2012, **20**, 20599.
14 Y. G. Liu, W. C. Choy, W. E. Sha and W. C. Chew, *Opt. Lett.*, 2012, **37**, 2112.
15 A. Devilez, B. Stout and N. Bonod, *ACS Nano*, 2010, **4**, 3390.
16 A. Ludwig, C. D. Sarris and G. V. Eleftheriades, *Phys. Rev. Lett.*, 2012, **109**, 223901.
17 R. C. Hansen, *Electrically small, superdirective, and superconducting antennas*, Wiley-Interscience, 2006.
18 R. E. Hansen, R. C.; Collin, *Small Antenna Handbook*, John Wiley and Sons Ltd, 2011.
19 A. D. Yaghjian, T. H. O′Donnell, E. E. Altshuler and S. R. Best, *Radio Science*, 2008, **43**, RS3002.
20 D. Scholnik and J. Coleman, *Proceedings of the 2001 IEEE Radar Conference*, 2001, 181 – 186.
21 D. S. Filonov, A. E. Krasnok, A. P. Slobozhanyuk, P. V. Kapitanova, E. A. Nenasheva, Y. S. Kivshar and P. A. Belov, *Appl. Phys. Lett.*, 2012, **100**, 201113.
22 B. Rolly, B. Stout and N. Bonod, *Optics Exp.*, 2012, **20**, 20376–20386.
23 A. E. Krasnok, A. E. Miroshnichenko, P. A. Belov and Y. S. Kivshar, *JETP Lett.*, 2011, **94**, 635.
24 A. B. Evlyukhin, S. M. Novikov, U. Zywietz, R. L. Eriksen, C. Reinhardt, S. I. Bozhevolnyi and B. N. Chichkov, *Nano Lett.*, 2012, **12**, 3749.
25 A. I. Kuznetsov, A. E. Miroshnichenko, Y. H. Fu, J. Zhang and B. Lukyanchuk, *Sci. Rep.*, 2012, **2**, 492.
26 Y. H. Fu, A. I. Kuznetsov, A. E. Miroshnichenko, Y. F. Yu and B. Lukyanchuk, *Nat. Comm.*, 2013, **4**, 1527.
27 B. Rolly, J.-M. Geffrin, R. Abdeddaim, B. Stout and N. Bonod, *Scientific Reports*, 2013, **3**, 3063.
28 M. W. Knight and N. J. Halas, *New J. Phys.*, 2008, **10**, 105006.
29 N. A. Mirin and N. J. Halas, *Nano Lett.*, 2009, **9**, 1255–1259.
30 Y. Zhang, N. K. Grady, C. Ayala-Orozco and N. J. Halas, *Nano Lett.*, 2011, **11**, 5519–5523.
31 L. Wollet, B. Frank, M. Schaferling, M. Mesch, S. Hein and H. Giessen, *Optic. Mater. Exp.*, 2012, **2**, 1384–1390.
32 A. Alu and N. Engheta, *IEEE Trans. on Antennas and Propagation*, 2007, **55**, 3027.
33 E. Palik, *Handbook of Optical Constant of Solids*, San Diego, Academic, 1985.
34 S. Boriskina, T. Benson, P. Sewell and A. Nosich, *IEEE J. Select. Topics*

Quantum Electron., 2006, **12**, 1175–1182.
35 Q. J. Wang, C. Yan, N. Yu, J. Unterhinninghofen, J. Wiersig, C. Pflugl, L. Diehl, T. Edamura, M. Yamanishi, H. Kan and F. Capasso, *PNAS*, 2010, **107**, 22407.
36 M. O. Scully, *PNAS*, 2010, **107**, 22367.
37 J. Y. Lee, B. H. Hong, W. Y. Kim, S. K. Min, Y. Kim, M. V. Jouravlev, R. Bose, K. S. Kim, I.-C. Hwang, L. J. Kaufman, C. W. Wong, P. Kim and K. S. Kim, *Nature*, 2009, **460**, 498.
38 Z. Wang, W. Guo, L. Li, B. Lukyanchuk, A. Khan, Z. Liu, Z. Chen and M. Hong, *Nat. Comm.*, 2011, **2**, 218.
39 L. H. Gabrielli and M. Lipson, *Opt. Expr.*, 2011, **19**, 20122.
40 A. D. Falco, S. C. Kehr and U. Leonhardt, *Opt. Expr.*, 2011, **19**, 5156.
41 D. Gerard, J. Wenger, A. Devilez, D. Gachet, B. Stout, N. Bonod, E. Popov and H. Rigneault, *Opt. Expr.*, 2008, **16**, 15297.
42 J. J. Schwartz, S. Stavrakis and S. R. Quake, *Nat. Nanotech.*, 2010, **5**, 127.
43 L. Robledo, L. Childress, H. Bernien, B. Hensen, P. Alkemade and R. Hanson, *Nature*, 2011, **477**, 574.
44 P. Siyushev, F. Kaiser, V. Jacques, I. Gerhardt, S. Bischof, H. Fedder, J. Dodson, M. Markham, D. Twitchen, F. Jelezko and J. Wrachtrup, *Appl. Phys. Lett*, 2010, **97**, 241902.
45 P. Ginzburg, N. Berkovitch, A. Nevet, I. Shor and M. Orenstein, *Nano Lett.*, 2011, **11**, 2329–2333.
46 J. Jackson, *Classical Electrodynamics*, New York : Wiley, 1998.
47 S. Sacanna, M. Korpics, K. Rodriguez, L. Colon-Melendez, S.-H. Kim, D. J. Pine and G.-R. Yi, *Nature Communication*, 2013, **4**, 1688.
48 S. Sacanna and D. J. Pine, *Current Opinion in Colloid & Interface Science*, 2011, **16**, 96–105.
49 S.-M. Yang, S.-H. Kim, J.-M. Lima and G.-R. Yi, *J. Mater. Chem.*, 2008, **18**, 21772190.
50 S. Sacanna, W. T. M. Irvine, L. Rossi and D. J. Pine, *Soft Matter*, 2011, **7**, 1631.
51 P. V. Dorpe and J. Ye, *ACS Nano*, 2011, **5**, 6774–6778.
52 B. Rolly, B. Stout, S. Bidault and N. Bonod, *Opt. Lett.*, 2011, **36**, 3368.
53 T. Pakizeh and M. Kall, *Nano Lett.*, 2009, **9**, 2343.
54 S. H. A. Lavasani and T. Pakizeh, *Opt. Lett.*, 2012, **29**, 1361.
55 Z. Liu, H. Lee, Y. Xiong and X. Zhang, *Science*, 2007, **315**, 1686.
56 Z. Jacob, L. V. Alekseyev and E. Narimanov, *Opt. Expr.*, 2006, **14**, 8247.
57 D. Lu and Z. Liu, *Nat. Comm.*, 2012, **3**, 1205.
58 F. J. Rodriguez-Fortuno, G. Marino, P. Ginzburg, D. OConnor, A. Martinez, G. A. Wurtz and A. V. Zayats, *Science*, 2013, **19**, 328–330.
59 P. B. Johnson and R. W. Christy, *Phys. Rev. B*, 1972, **6**, 4370–4379.